Effect of Solvent−Polymer Interaction in Swelling Dynamics of Ultrathin Polyacrylamide Films: A Neutron and X-ray Reflectivity Study

M. Mukherjee,*,† Amarjeet Singh,† J. Daillant,‡ Alain Menelle,§ and F. Cousin§

Surface Physics Division, Saha Institute of Nuclear Physics, 1/AF, Bidhannagar, Kolkata-700064, India, LIONS, Service de Chimie Moléculaire, bât. 125, CEA Saclay, F-91191 Gif-sur-Yvette Cedex, France, and Laboratoire Leon Brillouin, CEA Saclay, F-91191 Gif-sur-Yvette Cedex, France

Received August 2, 2006; Revised Manuscript Received December 8, 2006

ABSTRACT: The swelling dynamics of the ultrathin polyacrylamide (PAM) spin-coated films in saturated vapor of D_2O and H_2O were studied using neutron and X-ray reflectivity. A uniform scattering length density (SLD) profile represents the dry PAM films, whereas the SLD profiles corresponding to the swelled films were characterized with a decreasing solvent concentration along the film thickness from top surface to the film/substrate interface. The diffusion mechanism of D_2O into the films was found to be a non-Fickian process, as the D_2O diffusion coefficient was observed to be decreasing as a function of film thickness. The thickness dependent structural changes in the dry polymer films were suggested from the increased density of thinner films. The diffusion coefficient of polymer chains in the solvent on the contrary was independent of film thickness. The different nature of D_2O−PAM interaction (stronger) as compared to H_2O−PAM interaction was found to play a crucial role on the diffusion of polymer, where the diffusion coefficient of the chains was an order of magnitude higher in D_2O as compared to that in the H_2O. A lower value of the excluded-volume parameter in the case of D_2O also indicates stronger monomer−solvent interaction.

1. Introduction

When a dry polymer is exposed to a solvent, the solvent molecules enter into the porous structure of the polymer and diffuse into all accessible volume. If the polymer is soluble in the solvent, there is a strong attractive interaction between the polymer and the solvent and the net interaction between the polymer segments is repulsive. As a result the coiled polymer chains start to swell as soon as they are in contact with the solvent molecules. Eventually, the process leads to saturation where the swelled polymer chains are at thermodynamic equilibrium with the solvent.[1] The understanding of polymer chain dynamics and their equilibrium structure near surfaces and interfaces in presence of solvents are very important for their usage in polymer coatings, adhesion, emulsion and device applications.[2−9] A substantial amount of literature is available on the chain conformations, the thermal diffusion and glass transition of the ultrathin polymer films supported on solid surfaces.[10−17] Most often, the polymers chosen for those studies were insoluble in water. On the other hand systematic observations with ultrathin polymer films of water-soluble polymers are not available in the literature until recently[1,6,7] though they have broad range of applications such as biomaterials, biosensors, and preservation of foods.[18−22] In this article, we discuss the swelling dynamics of ultrathin films of polyacrylamide (PAM), a water-soluble linear chain homopolymer, in presence of the saturated D_2O and H_2O vapor using neutron and X-ray reflectivity. Here our objective was to study the effect of solvent−polymer interaction on the swelling dynamics through the application of solvents of slightly different nature. In a recent study with polymer nanocomposites, we have observed that the interaction between the nanocrystalline CdS particles and the polymer plays very significant role in the swelling dynamics,[6] which motivates us to carry out the present investigation. The main advantage of the neutrons as a probe is the large contrast between the scattering cross sections of ^1H and ^2D which allows us to observe the solvent (D_2O) distinctly in a hydrogen containing polymer environment. This property of neutrons has been extensively utilized for solving problems like polymer chain conformations, polymer mixing and the structure of liquids at surfaces by selective deutration.[10,11,23−27]

In our experimental study using neutron reflectivity, we have mainly used D_2O as the solvent to study the swelling dynamics of ultrathin PAM films. The large scattering density contrast between D_2O and PAM allows us to precisely follow the swelling[1,6] of the films in a time-resolved experiment as a function of D_2O exposure time. The mass densities of D_2O and bulk PAM being very close, we could follow the mass uptake simultaneously under the same experimental condition unlike our earlier X-ray reflectivity study[1] where mass uptake was measured separately using a gravimetric technique. To compare the polymer dynamics in H_2O vapor we have used X-ray reflectivity since neutron reflectivity did not allow us to follow the swelling at all times. Here we discuss three important observations of the present study: (a) nonuniform solvent concentration along the depth of the films; (b) the D_2O mass uptake behavior of the polymer films, which is film thickness dependent due to the compaction of the films with lowering of thickness; (c) the polymer chain dynamics in D_2O vapor, which is almost an order of magnitude faster when compared to their dynamics in H_2O.

2. Experimental Section

2.1. Sample Preparation. Polyacrylamide (PAM), a water-soluble polymer, with a molecular weight of 5×10^6 (degree of polymerization $N = 70\,422$) was procured from Polysciences, Inc. An aqueous solution of PAM was used to prepare ultrathin films coated on silicon substrates using the spin-coating technique[29]

† Surface Physics Division, Saha Institute of Nuclear Physics.
‡ LIONS, Service de Chimie Moléculaire, bât. 125, CEA Saclay.
§ Laboratoire Leon Brillouin, CEA Saclay.

10.1021/ma061745d CCC: $37.00
Published on Web 01/26/2007

Table 1. Scattering Length Densities (SLD) of the Materials Used in Our Experiment

material	scattering length density ρb (10^{-7})	mass density at 25 °C (g/cm^3)
H_2O	−5.6	1.0
D_2O	63.9	1.1
Si	20.5	2.33
PAM (bulk)[37]	15.6	1.12

(spin-coater, Headway Research Inc., EC 101). To make the surface suitably hydrophilic for coating of water-soluble polymers, polished silicon substrates with 2 in. diameter and 1 mm thickness were chemically treated with a mixture of ammonia solution and hydrogen peroxide (NH_4OH:H_2O_2:H_2O = 1:1:2) at boiling temperatures for 5 min before spin-coating on them. During the spinning, clean and warm air (60 °C) was passed gently over the sol using a homemade arrangement to facilitate a faster evaporation of water. The thicknesses of the films were controlled by varying the spinning speed (600−2000 rpm) of the rotating substrate and also by changing the initial sol concentration (2.0−6.0 mg/mL). A set of films with different thicknesses (100, 267, 487, and 725 Å, measured from neutron reflectivity) was prepared. It is generally believed that the spin-coated films with high spinning speed may remain in a nonequilibrium structure. The films were kept for 30 min in a closed container at saturated water vapor pressure at room temperature. Since the polymer was water-soluble, the films absorbed water vapor to swell and as a result the strain was released and the films attained equilibrium structures.

2.2. Neutron and X-ray Reflectivity Measurements. The refractive index of a material for neutrons and X-rays can be described by a single equation

$$n = 1 - \delta - i\beta \tag{1}$$

where δ and β represent the scattering strength and the absorption of the material respectively. In the case of X-rays, $\delta_X = \lambda^2\rho_{el}r_0/2\pi$ and $\beta_X = \mu\lambda/4\pi$, where λ is X-ray wavelength, ρ_{el} is the electron density, r_0 is classical electron radius (2.82×10^{-5} Å), and μ is the linear absorption coefficient. In the case of neutrons for nonmagnetic materials, $\beta_N \approx 0$ and $\delta_N = \lambda^2\rho bN_A/2\pi M$, where ρ is the density and M is the molecular weight of a monomer unit having a scattering length of b, which is sum over all nuclei in the monomer.[23,24] The basic difference between neutron and X-ray reflectivity arises due to their interaction with the material, X-ray photons interact with the electrons in the sample, whereas neutrons interact with the nucleus. In most cases the neutron absorption can be neglected in comparison to the X-ray absorption. The materials of different electron densities produce scattering contrast for X-rays, whereas for neutron the scattering contrast is produced due to the difference in the scattering length densities (SLD) of the materials. The SLD of an element is defined as the density ρ multiplied with scattering length of the element b. The calculated values of scattering length densities of different materials (H_2O, D_2O, PAM, and Si) used in this experimental study are listed in Table 1.

Neutron reflectivity data were collected using time-of-flight reflectometer EROS at LLB in France. The time-of-flight is a wavelength dispersive technique. This technique consists in sending a pulsed white beam on the sample and measuring the "time-of-flight" of neutrons traveled from source to detector for each wavelength in the spectrum. Since the speed of neutrons varies as the inverse of the wavelength, the latter is directly related to the time taken by the neutron to travel from the pulsed source to the detector. For the reflectivity measurement, the angle (θ) between the incident neutron beam and the sample surface is kept fixed and the data are obtained by measuring reflected beam counts for each wavelength of the available spectrum, where the available range of the neutron wavelength (λ) varies from 3.5 − 22 Å with fixed $\Delta\lambda \sim 0.15$ Å. Only a limited range of wave-vector space ($q_z = 4\pi/\lambda(\sin\theta)$) is accessible for reflectivity measurements for the given wavelength range. To scan the large wave-vector space, the data can be collected at several fixed angles. At first, the samples (PAM films) were mounted in a sample-chamber designed to have Kapton windows for the entrance and exit of the neutron (X-ray) beams. The schematic arrangement of the neutron reflectivity experiment with sample-chamber is shown in Figure 1. The samples were aligned at fixed angle $\theta = 0.93°$ and were heated at 105 °C for 30 min under vacuum (10^{-3} Torr) to expel the moisture trapped in the polymer films. The samples were then cooled to a fixed temperature 26 °C which was 4 deg above the temperature of neutron hall (22 °C) and the reflectivity data of the dry PAM films were collected. To study the swelling of polymer films the chamber was opened and a small tub of D_2O was quickly inserted (as shown in Figure 1), which was again closed tightly to yield a saturated vapor inside. The time of insertion of the solvent in the chamber was noted as the starting point of the exposure time ($t = 0$). The films start to swell as soon as they are exposed to the solvent vapor (D_2O). The reflectivity scans were immediately started after the exposure to continuously monitor the film thickness in successive intervals. The data acquisition time varied from 5 to 30 min for each thickness, which was sufficient to have reasonably good statistics. After the film thickness attains saturation value, the incident angle was changed to 2.5 deg to collect the reflectivity data in a larger wavevector range.

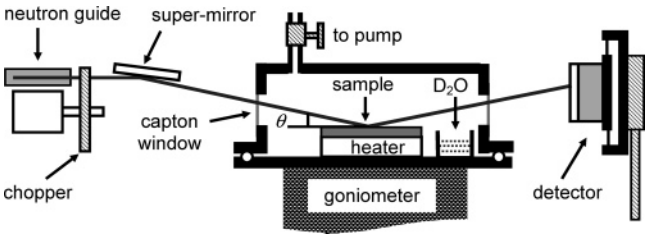

Figure 1. Schematic arrangement of the neutron reflectivity experimental setup along with the sample-chamber at a fixed incident angle (θ).

The same set of polymer films was used to study the swelling dynamics in H_2O vapor using X-ray reflectivity to compare with their dynamics in D_2O vapor. Neutron reflectivity could not be used for this purpose since the presence of H_2O in PAM films equalizes the scattering length densities of the films and Si substrates hence no oscillations are observed at the intermediate stage of swelling, which we shall discuss later in section 3.2. X-ray reflectivity data were collected using an angle dispersive X-ray diffractometer (Bruker AXS, Germany, D8 Discover) with a fixed wavelength (Cu Kα) sealed tube X-ray source followed by Göbel mirror (Ni/C) to collimate Cu Kα radiation. The polymer films were mounted in the sample-chamber and were heated at 105 °C under vacuum (10^{-1} Torr) for 30 min to expel the moisture. The sample temperature was then set to 26 °C and the room temperature was maintained at 22 °C (The stability of the room temperature was not as good as that of the neutron hall, the actual room-temperature went slightly higher for some measurements). It may be noted that due to higher chamber pressure the initial thickness obtained from X-ray reflectivity measurement for the same set of films were about 15% higher (115, 305, 566, and 818 Å). To study the swelling of polymer films, the chamber was opened and a small tub of H_2O was quickly inserted and the chamber was again closed tightly to have a saturated vapor inside. The films start to swell when they are exposed to the solvent vapor. The film thickness was continuously monitored using X-ray reflectivity in successive intervals. The data acquisition time for each scan was 7−10 min for different films, which was adjusted to have reasonably good statistics for a selected wavevector range.

2.3. Data Analysis. The neutron and X-ray reflectivity data were analyzed using the recursive multilayer method[23,24] originally formulated by Parratt.[30] In this formalism, a reasonable input model based on the prior knowledge of the specimen is used in a fitting program, which minimizes the deviation between the experimental data and the calculated reflectivity profiles based on the input model. In the case of neutron reflectivity, the resolution broadening (Δq_z) was an increasing quadratic function of wavevector q_z, whereas in

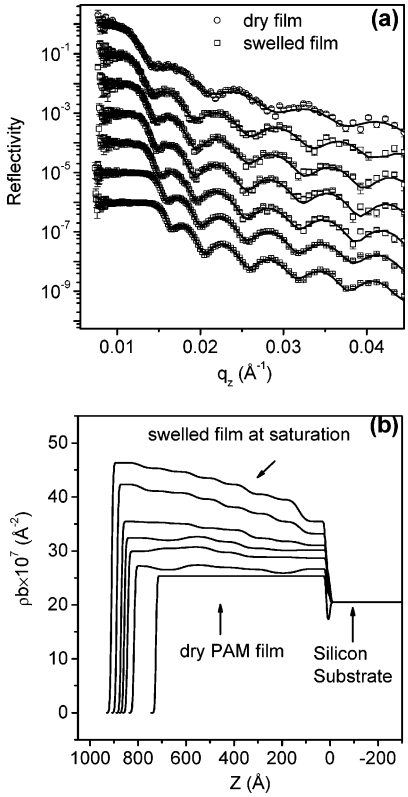

Figure 2. (a) Neutron reflectivity data (symbols) with fitted profiles (lines) of the swelling polymer films when exposed to D_2O, from top to the bottom as a function of increasing exposure time. (b) Scattering length density (SLD) profiles corresponding to the reflectivity data.

the case of X-ray reflectivity there was a constant resolution broadening for the entire wavevector range therefore the resolution function was modified accordingly in the code. In our analysis, the total thickness of the films were divided into several layers with finite interfacial roughness. The thickness of the layers were kept more than the depth resolution ($2\pi/q_z^{max} \sim 100$ Å, where q_z^{max} is the maximum value of q_z for a given reflectivity data) and the maximum interfacial roughness allowed in the fittings were less than one-fourth of the thickness of the each layer. The parameters obtained from the fitting provide the information regarding the total film thickness, roughness at the interfaces and the scattering length density (SLD) profile (electron density profiles in the case of X-rays) along the film thickness.

3. Results and Discussion

3.1. D_2O Mass Transport into the Films. In Figure 2, the neutron reflectivity data along with the observed SLD profiles of a typical polymer film (725 Å) are plotted for dry and at various stages of swelling after they were exposed to D_2O vapor. It can be seen in Figure 2b that the entire dry PAM film can be represented by a single SLD with a small dip near the film/substrate interface occurring due to the lower anchoring chain density as observed earlier.[7] After exposure to D_2O, the films swell continuously as a function of exposure time and eventually attain a saturation value. The SLD profiles corresponding to the swelled films are characterized with a decreasing value from top surface to the film/substrate interface as observed in Figure 2b. Since the scattering length density of D_2O is very large as compared to the polymer films, the gradient in the SLD profile signifies that the concentration of D_2O is highest at the air/film interface which gradually reduces to the lowest value at film/substrate interface. The neutron reflectivity data and the corresponding SLD profile of the film swelled in D_2O vapor is compared with those for the SLD profile of the same film

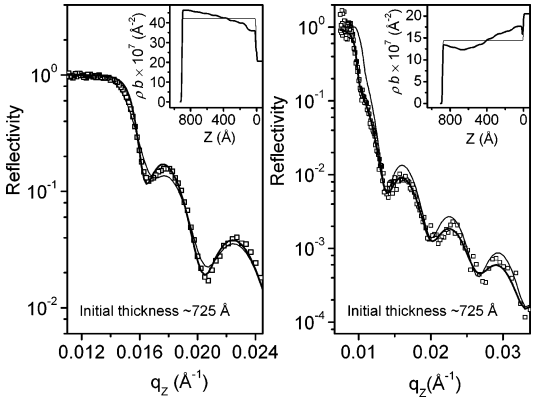

Figure 3. Neutron reflectivity data (symbols) of a swelled PAM film (725 Å) in presence of D_2O vapor (left panel) and in presence of H_2O vapor (right panel). The observed model profiles are shown in the insets of the respective panels. The thick solid lines (best fits to the data) represent the model profiles characterized with the density gradient along the depth. The flat density profiles and the corresponding reflectivity results (thin line) are shown to highlight the mismatch.

swelled in H_2O vapor in Figure 3. It can be observed that the average SLD of the swelled film in H_2O vapor is lower than that of silicon and the SLD profile increases from top surface to the film/substrate interface, which are opposite to the trends observed in the case of swelling in D_2O. Since the scattering length density of H_2O is negative (see Table 1) its presence in the film contributes to reduce the average SLD of the film. The lower value of SLD at the top surface as compared to the value at the film/substrate interface indicates the concentration of H_2O is largest at the top, which then gradually reduces along the depth of the film. The higher concentration of solvent at the top surface which gradually decreases toward the bottom (polymer/silicon interface) for both the cases indicates a nonuniformity in the swelling of the films along the thickness. It may be noted that the polymer segments at the top surface are free whereas at polymer/silicon interface the attractive polymer−substrate interaction hinders the motion of the segments that are attached to the substrate. Therefore, in presence of solvent the segments near the top surface of the films are likely to swell more than those near the substrate giving rise to the concentration gradient of the solvent in the films.

It can be clearly observed from Figure 2 that in addition to the increase in the thickness there is a systematic enhancement of SLD as a result of swelling in D_2O vapor. Since the SLD of D_2O is very large as compared to that of PAM (see Table 1), the presence of a small fraction of D_2O in the PAM films can be detected by neutrons. Therefore, the overall scattering length density, which is the weighted average of both the components (D_2O and PAM), increases systematically as a function of exposure time. The continuous transport of D_2O molecules into the film and their observation by neutron reflectivity in a time-resolved experiment can be utilized to describe the solvent profile in the polymer films using the relation for the SLD of the composites as $\rho_{comp} = c_{D_2O}\rho_{D_2O} + (1 - c_{D_2O})\rho_{PAM}$ in terms of the concentration, c_{D_2O} of pure D_2O. In Figure 4, we have shown the derived D_2O profiles as a function of time for all the film. It can be clearly observed that the solvent profile is initially flat and with higher solvent availability the top surface swells more that the one attached to the substrate. This may be interpreted in terms of fact that the polymer chains that are attached to the substrate have less degree of freedom as compared to those at the free top surface. The integrated area under the solvent profiles of Figure 4 represents the solvent mass uptake as a function of time, A_t. In the top panel of Figure

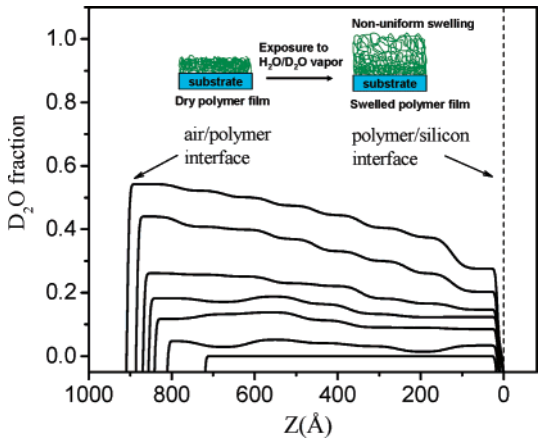

Figure 4. Fraction of D_2O in the film (725 Å) at different exposure times obtained from the profiles in Figure 2b using the relation $\rho_{comp} = c_{D_2O}\rho_{D_2O} + (1 - c_{D_2O})\rho_{PAM}$. The cartoon in the inset depicts the nonuniform swelling.

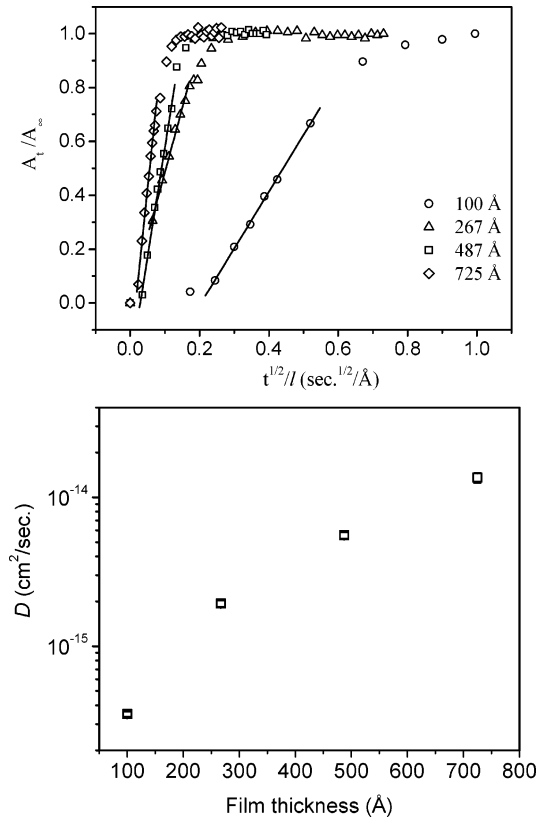

Figure 5. Top panel: Normalized mass uptake in terms of integrated SLD ratio (see text) against square root of time scaled with film thickness. Initial thickness of the films is shown against the symbols. A_t and A_∞ are the areas under D_2O profile (ref Figure 4) at time t and saturation area respectively. The lines represent the linear fit in the initial region. Bottom panel: Diffusion coefficient of D_2O as a function of initial film thickness (100, 267, 487, 725 Å).

5 we have plotted the ratio of these areas to the saturated area A_∞ as a function of square root of time scaled by the dry film thickness for all the films. It is clearly observed from the figure that the curves corresponding to the films of different thickness l do not coincide, indicating thickness dependent diffusion mechanism. In other words, the process governing the diffusion of D_2O into the PAM films was non-Fickian[28] in nature. The slope of the linear region of these curves have been used to obtain the diffusion coefficients of the solvent using the Fickian diffusion formula,[8,28] $M_t/M_\infty = (2/l)(Dt/\pi)^{1/2}$, where M_t/M_∞., the ratio of the mass uptake of the films at different times is equal

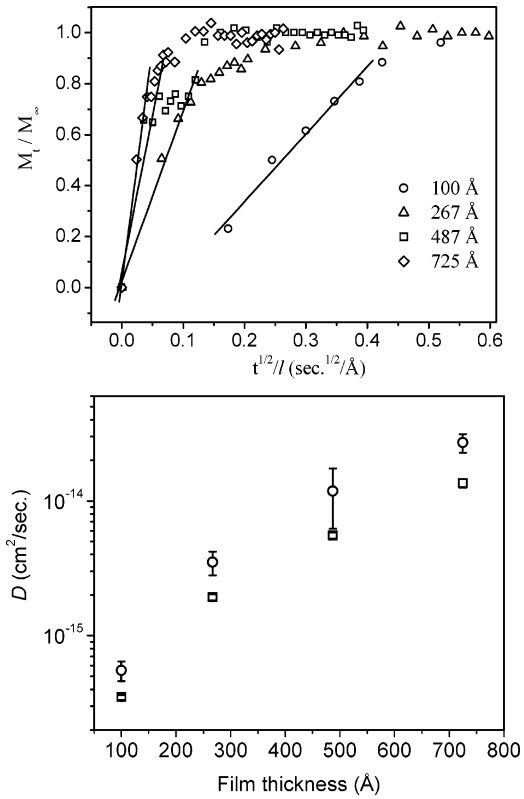

Figure 6. Top panel: Normalized mass uptake against square root of time scaled with film thickness. Initial thickness of the films is shown against the symbols. The lines represent the linear fit in the initial region. Bottom panel: Diffusion coefficient (circle) of D_2O as a function of initial film thickness (100, 267, 487, 725 Å) as compared to the diffusion coefficient (square) in Figure 5.

to the ratio of the integrated area profiles A_t/A_∞. The diffusion coefficients obtained from the data have been plotted in the bottom panel of Figure 5 for all the films.

It is interesting to note that the densities of PAM and D_2O are almost equal. In this situation mass of the film at time t can be expressed as $m_t = \rho A L_t$ where ρ is the mass density, A is the area and l_t is the thickness of the films at time t. Since the area of the film remains unchanged during swelling (see section 3.2), the mass uptake defined as $M_t = (m_t - m_0)/m_0$, where m_t is the mass of the film at time t and m_0 is the initial mass, may also be written in terms of film thickness at different times as $M_t = (l_t - l_0)/l_0$, where l_0 is the initial film thickness. In the top panel of Figure 6, typical normalized mass uptake M_t/M_∞ is shown against $t^{1/2}/l$ for all the films, where M_t is the mass uptake at time t and M_∞ represents saturated mass uptake. The diffusion coefficients for all the film were calculated using the linear regions of the curves using the Fickian diffusion formula as described above. The diffusion coefficients obtained from this method have been compared with the numbers obtained from the previous method in the bottom panel of Figure 6. The close agreement between the two sets of results indicates that the solvent profiles obtained from the neutron scattering method were very accurate. Here we have observed that the diffusion coefficient increases systematically with the increase in film thickness. It may be noted that in our earlier X-ray reflectivity study[1] with PAM systematic thickness dependence in solvent diffusion could not be observed within the experimental resolution, possibly due to the narrow range of film thickness (210−450 Å) used in that experiment. However, in another study with a CdS−PAM nanocomposite with a larger range of thickness, a thickness dependent diffusion coefficient was observed where the effect was explained in terms of restricted

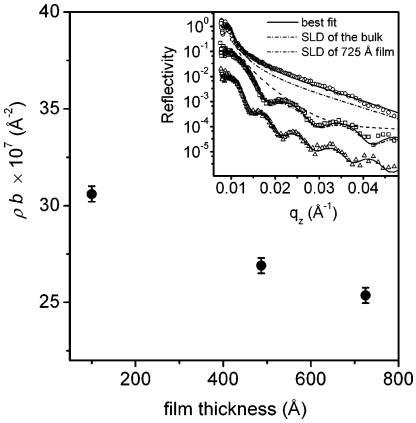

Figure 7. Scattering length density as a function of initial film thickness (100, 487, 725 Å). The inset shows the neutron reflectivity data (along with the fittings for different profiles to justify the requirement of different densities for different films) of the films: 100 (circle), 487 (square) and 725 Å (up-triangle).

diffusion of polymer chains due to confinement.[6] Here also we explain the reduction of diffusion coefficient with film thickness during mass uptake in terms of the thickness dependent structural changes in these films. In Figure 7, the average scattering length densities of the dry PAM films obtained from the neutron reflectivity data analysis (shown in the inset) are plotted against the initial thickness of the films except for one film (267 Å).[31] It can be observed from the figure that the SLD of the thinner films are higher than those of the thicker ones and approaches toward that of the bulk PAM value when the thickness increases. The increase in the SLD of the films indicates the change in the internal structure of the films due to the confinement of the chains between the interfaces. The alignment of the polymer segments along the substrate plane enhances the packing density of the chains as compared to the bulk polymer where chains are randomly oriented. As a result of this ordering, the diffusion channels are more aligned in the two dimensions with lowering of their diameters; hence, the diffusion of the solvent into these channels the films is hindered in thinner films in comparison to the thicker ones where the orientation of the diffusion channel are more random.

3.2. Swelling Dynamics of Polymer Chains. The diffusion of the polymer chains during swelling or thermal motion of the thin polymer films coated on substrates are observed to occur only along the direction perpendicular to the substrate due to the physical restriction in the other two in-plane dimensions.[1,6,13,14] As discussed earlier[1] for the analysis of the swelling dynamics of thin polymer films the end-to-end distance $R(t)$ of a single free chain at time t in one dimension is described with the initial condition $R(t=0) = R_0$ as[1,32]

$$R(t) = \mathrm{e}^{-(2D/N)t}\left[R_0^{\,3} + \frac{\upsilon N^3}{2}(\mathrm{e}^{6(D/N)t} - 1)\right]^{1/3} \qquad (2)$$

where D is the diffusion coefficient of the polymer chains, N is the degree of polymerization, and υ is the excluded volume parameter which is a positive quantity for swelling and determines the saturated thickness of the films. When the polymer film thickness is less than R_g, it is generally assumed that the films are constructed from side by side placement of a single layer of individual polymer coils that are flattened by substrate interaction.[33] It is assumed that in presence of solvent each individual macromolecule swells independently. Although the polymer chains are not truly free as they are mutually entangled and also bonded to the substrate, the above equation represent the swelling dynamics of the polymer films very accurately since the strong hydrophilic interactions between the solvent and the polymer molecules dominates the swelling dynamics.

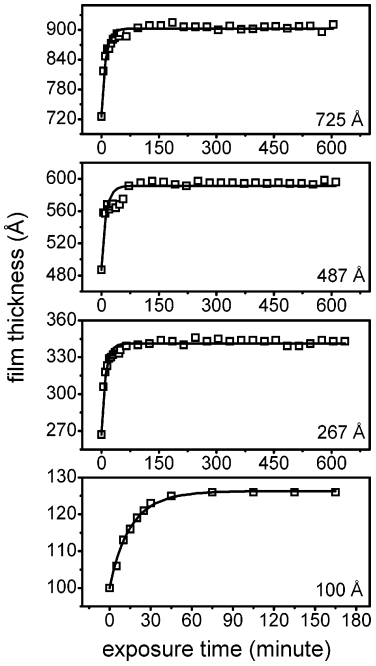

Figure 8. Swelling of the films as they are exposed to the saturated D_2O vapor. Symbols represent the experimental data (obtained from neutron reflectivity) and lines are obtained by fitting the data using eq 2. The initial thickness of the films are shown in the respective panels.

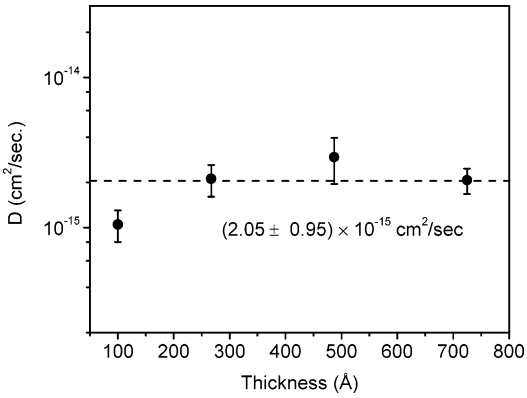

Figure 9. Diffusion coefficients of polymer chains in D_2O vapor as a function of initial film thickness (100, 267, 487, 725 Å) obtained from neutron reflectivity. The dotted line indicates the average value.

In Figure 8, we have plotted the thickness of four different films obtained from neutron reflectivity measurement as a function of exposure time. To find the diffusion coefficients of polymer chains the observed thickness of the films were fitted with eq 2, where the data are in excellent agreement with the equation. The diffusion coefficients obtained from the fittings are plotted as a function of film thickness in Figure 9. It can be observed that there is no systematic dependence of the diffusion coefficients on the film thickness. A dashed line in the figure represents the average value (2.05×10^{-15} cm^2/s) of the diffusion coefficients of polymer chains in presence of D_2O vapors, which is almost an order of magnitude higher than the value reported earlier (3.2×10^{-16} cm^2/s) in the case of swelling dynamics of the PAM films in H_2O.[1] We believe that the difference in the diffusion coefficients occurs due to the difference in the nature of interaction of the two solvents (H_2O and D_2O). To reaffirm these observations we performed the

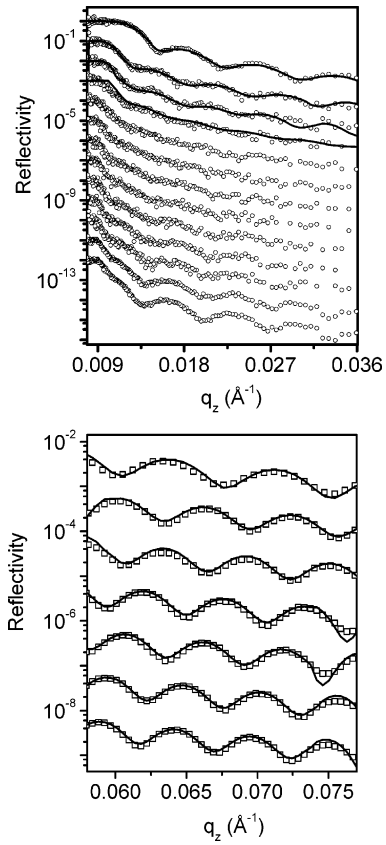

Figure 10. Neutron reflectivity data (top panel) and X-ray reflectivity data (bottom panel) of the swelling polymer films when exposed to the saturated H_2O vapor, from top to bottom as a function of increasing exposure time. The solid lines represent fits to the reflectivity data in each panel.

swelling experiments with a particular film (725 Å) in the saturated vapor of H_2O using neutron reflectivity, and the observed data are plotted in the top panel of Figure 10. It can be observed that the reflectivity oscillations gradually smear out on exposure to H_2O and the same could not be observed during intermediate stage of swelling, which again appear gradually toward the saturation. The SLD of silicon is slightly less than that of PAM and the negative contributions of H_2O bring the SLD of the swelled film close to that of silicon. As a result of loss of contrast in SLD, the reflectivity oscillations could not be observed in the large intermediate range of exposure time. In the final stage of the swelling when the amount of H_2O in the film was sufficient to produce scattering contrast with the substrate, the reflectivity oscillation reappeared as expected. It may be noted that the curvature of the data plays the key role by using eq 2 from the swelling data in determining the diffusion coefficient; hence, nonavailability of good data in this vital region hinders accurate predictions by neutron reflectivity method. However we have used the initial four data (at later stage, due to failure in temperature controller, the thickness became unreliable) and the average excluded volume parameter (obtained from X-ray reflectivity experiment) to calculate the diffusion coefficient of polymer chains in H_2O vapor. The data fitting and the obtained value are shown in Figures 11 and 12 respectively. However it was clear that the neutron reflectivity method was not suitable to monitor the swelling of polymer films in presence of H_2O vapor. We have also used X-ray reflectivity to monitor the swelling of the same set of films in saturated H_2O vapor. The observed X-ray reflectivity data along with the fittings are shown in the bottom panel of Figure 10.

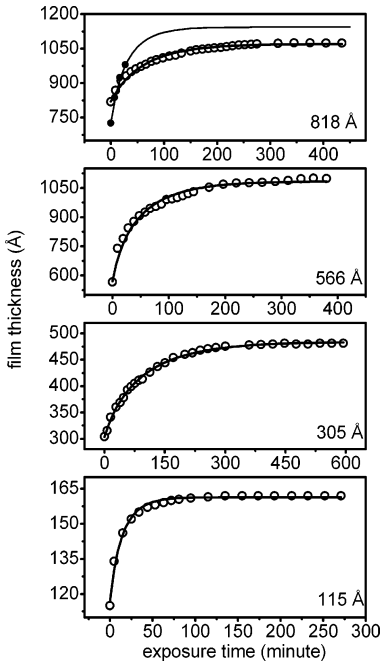

Figure 11. Swelling of the films as they are exposed to saturated H_2O vapor. The film thickness was monitored using X-ray reflectivity as a function of exposure time. Symbols represent experimental data, and the lines are obtained by fitting the data using eq 2. The initial thicknesses of the films are shown in the corresponding panels. Four solid symbols in the top panel shows the neutron reflectivity data and the line (extended up to saturation thickness) represents the best fit to eq 2 using average excluded parameter (2.25×10^{-14}) from X-ray reflectivity experiment.

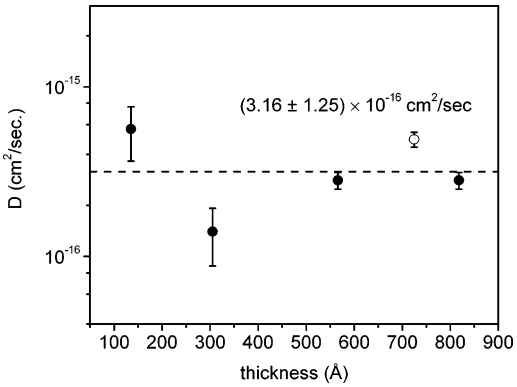

Figure 12. Diffusion coefficients of polymer chains in saturated H_2O vapor as a function of initial film thickness (115, 305, 566, 818 Å) obtained from X-ray reflectivity. Dotted line indicates the average value. An open circle represents the diffusion coefficient obtained from neutron reflectivity data.

In Figure 11, the thickness of the films during swelling as obtained from X-ray reflectivity measurements of the different polymer films are plotted as a function of exposure time. It may be noted that the initial thickness of all the films were observed to be about 15% higher than the earlier values due to the lower capacity of the diaphragm vacuum pump ($\sim 10^{-1}$ Torr) used for drying the films during X-ray reflectivity measurement. To calculate the polymer diffusion coefficients, the swelling data of the films were fitted with eq 2 as shown in Figure 11. The diffusion coefficients obtained from the fittings are plotted as a function of initial film thickness in Figure 12. No systematic thickness dependence in the diffusion coefficients was observed and the average value (3.16×10^{-16} cm^2/s) was in close agreement with our earlier reported number. These observations

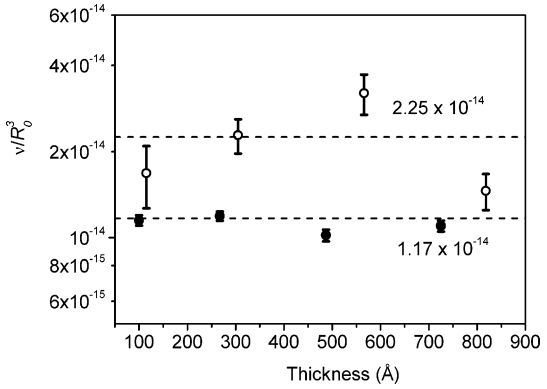

Figure 13. Normalized excluded volume parameter of the films in D_2O (solid symbol) and in H_2O (open symbol) as a function of film thickness. Dotted lines indicate the average values.

reveal that there is a clear distinction in the swelling dynamics of polymer chains in the two solvents. Though D_2O and H_2O are chemically identical, a difference in their physical nature of interaction was observed earlier,[34] where the solubility of a protein (lysozyme) in H_2O was found to be 1.3 times the solubility in D_2O. We also have similar indications from the volume fraction of the solvent in the films after the saturation thickness was attained. The volume fraction of the solvent defined as $\phi_s = (t_f - t_i/t_f)$ was calculated for H_2O and D_2O, where t_i and t_f are the initial and the final thickness of the films. The values of ϕ_{D_2O} and ϕ_{H_2O} were calculated for all the films, which were observed to be 0.20 ± 0.02 and 0.36 ± 0.1 respectively. A higher degree of hydrogen bonding in D_2O compared to H_2O was reported earlier,[35] and we believe the same plays very critical role in the observed difference of swelling dynamics of polymer molecules in presence of the two vapors. The swelling dynamics of polymer chains are observed to be faster when the solvent−polymer interaction was comparatively stronger. The excluded volume parameters obtained from the fitting of the data are plotted after normalization by dividing them with the cube of the corresponding film thickness in Figure 13. It can be clearly observed that average normalized excluded-volume (ν/R_0^3) in the case of swelling in H_2O vapor is large compared to that in D_2O vapor, which is commensurate with the higher value of ϕ_{H_2O} as compared to ϕ_{D_2O}. The excluded volume parameter $\upsilon = (1 - 2\chi)a^3$ is responsible for the swelling, where $\chi = \chi_{MS} - 1/2(\chi_{MM} + \chi_{SS})$ and a is the monomer dimension. The subscripts MS, MM, and SS denote the monomer−solvent, monomer−monomer, and solvent−solvent interactions respectively.[33,36] In Figure 12, we can clearly observe that the normalized excluded volume parameters for swelling in D_2O is slightly lower compared to the swelling in H_2O (although the H_2O data appears to be scattered due to the fluctuation of the room temperature during X-ray reflectivity measurements). It may be noted that the expression of χ consists of two terms χ_{MS} and χ_{SS} that are related to the solvent. The lower value of ν in the case of D_2O may be explained in terms of the increase of both the solvent related parameters with the monomer−solvent term dominating over the solvent−solvent term.

4. Conclusion

In conclusion, the mass uptake and swelling dynamics of the ultrathin polyacrylamide films were simultaneously observed using neutron reflectivity. The dry polymer films were characterized with uniform density throughout the film with a small dip near film/substrate interface representing low anchoring density. The SLD profiles of the swelled films were observed to possess a density gradient along the direction of film thickness, which indicate a decreasing solvent concentration from the top surface of the film to the film/substrate interface. The occurrence of solvent concentration gradient was attributed to the restricted swelling of the chains at the film/substrate interface as compared to the free swelling at the top surface (air/film interface). The D_2O mass uptake of the polymer films was observed to be a thickness dependent process, which is a non-Fickian transport. The lowering of the diffusion coefficient of D_2O with the film thickness was attributed to the compaction of the films as a result of confinement of the polymer chains. This was supported by the fact that the SLD of the dry films were larger than that of the bulk polymer with their systematic increase with lowering of the film thickness. The swelling dynamics of the polymer films were observed to be independent of the film thickness. A difference in the nature of interaction of D_2O and H_2O was observed to have a significant role on the swelling dynamics, as the polymer diffusion coefficient in D_2O was an order of magnitude larger than the same in the case of H_2O. The faster diffusion of polymer chains in D_2O was explained in terms of stronger D_2O−PAM interaction as compared to H_2O−PAM interaction as a result of higher degree of hydrogen bonding in D_2O. The lower value of excluded-volume parameter in the case of D_2O was explained in terms of the increase of monomer−solvent and solvent−solvent interaction with the monomer−solvent term dominating over the solvent−solvent term.

Acknowledgment. The authors thank Christian Blot for his assistance during the experiments at LLB.

References and Notes

(1) Singh, A.; Mukherjee, M. *Macromolecules* **2003**, *36*, 8728.
(2) Baer, D. R.; Burrows, P. E.; El-Azab, A. A. *Prog. Org. Coat.* **2003**, *47*, 342.
(3) Jones, R. A. L.; Richards, R. W. *Polymers at Surfaces and Interfaces*; Cambridge University Press: London, 1999.
(4) Witten, T. A.; Pincus, P. A. *Structured Fluids*; Oxford University Press: New York, 2004.
(5) Daoud, M.; Williums, C. E. *Soft Matter Physics*; Springer-Verlag: Berlin and Heidelberg, Germany, 1999.
(6) Singh, Amarjeet;, Mukherjee, M. *Macromolecules* **2005**, *38*, 8795.
(7) Singh, Amarjeet;, Mukherjee, M. *Phys. Rev. E* **2004**, *70*, 051608.
(8) Bosch, P.; Fernandez, A.; Salvador, E. F.; Corrales, T.; Catalina, F.; Peinado, C. *Langmuir* **2004**, *20*, 1453.
(9) Hamers, R. J. *Nature (London)* **2001**, *412*, 489.
(10) Jones, R. L.; Kumar, S. K.; Ho, D. L.; Briber, R. M.; Russell, T. P. *Nature (London)* **1999**, *400*, 146.
(11) Kraus, J.; Muller-Buschbaum, P.; Kuhlmann, T. D.; Schubert, W.; Stamm, M. *Europhys. Lett.* **2000**, *49*, 210.
(12) de Gennes, P. G. *Eur. Phys. J. E* **2000**, *2*, 201.
(13) Orst, W. J.; van Zanten, J. H.; Wu, W. L.; Satija, Sushil, K. *Phys. Rev. Lett.* **1993**, *71*, 867.
(14) Mukherjee, M.; Bhattacharya, M.; Sanyal, M. K.; Geue, Th.; Grenzer, J.; Pietsch, U. *Phys. Rev. E.* **2002**, *66*, 061801.
(15) Kajiyama, T.; Tanaka, K.; Satomi, N.; Takahara, A. *Macromolecules* **1998**, *31*, 5150.
(16) Miyazaki, T.; Nishida, K.; Kanaya, T. *Phys. Rev. E.* **2004**, *69*, 022801.
(17) Miyazaki, T.; Nishida, K.; Kanaya, T. *Phys. Rev. E.* **2004**, *69*, 061803.
(18) Fair, B. D.; Jamieson, A. M. *J. Colloid Interface Sci.* **1980**, *77*, 525.
(19) Chan, B. M. C.; Brash, J. L. *J. Colloid Interface Sci.* **1984**, *82*, 217.
(20) Arnebrant, T.; Nylander, T. *J. Colloid Interface Sci.* **1986**, *111*, 529.
(21) Rames, A.; Williums, D. F. *Biomaterials* **1992**, *13*, 731.
(22) Green, R. J.; Hopkinson, I.; Jones, R. A. L. *Langmuir* **1999**, *15*, 5102.
(23) Daillant, J.; Gibaud, A. *X-Ray and Neutron Reflectivity: Principles and Applications*, Springer: Berlin, 1999.
(24) Russell, T. P. *Materials Science Reports*; Elsevier Science Publ.: Amsterdam, 1990; Vol. 5.
(25) Lin, E. K.; Kolb, R.; Satija, S. K.; Wu, W. L. *Macromolecules* **1999**, *32*, 3753.

(26) Lee, L. T.; Langevin, D. Farnoux, B. *Phys. Rev. Lett.* **1991**, *67*, 2678.
(27) Penfold, J. E.; Lee, M.; Thomas, R. K. *Mol. Phys.* **1989**, *68*, 33.
(28) Crank, J.; Park, G. S. *Diffusion in Polymers*; Academic Press: London, 1968.
(29) Lawrence, C. J. *Phys. Fluids* **1988**, *31*, 2786.
(30) Parratt, L. G. *Phys. Rev.* **1954**, *98*, 359.
(31) We have obtained a very low value (17.0×10^7 Å^{-2}) for the dry scattering length density of the film (267 Å) since a test swelling experiment was performed with the film in saturated vapor of H_2O using X-ray reflectivity before the actual experiment with neutrons. The film remained in the saturated H_2O vapor for almost 6 h and the heating of the film at 105 °C for 30 min prior to the neutron study was not sufficient to dry the film. A similar result was observed when a film swelled in D_2O vapor was heated in vacuum for the second time. The scattering length density observed this time was much higher (33.0×10^7 Å^{-2}) than their earlier value (24.0×10^7 Å^{-2}) due to the presence of D_2O in the film.
(32) Pitard, E.; Bouchaud, J. P. *Eur. Phys. J. E* **2001**, *5*, 133.
(33) de Gennes, P. G. *Scaling concepts in polymer physics*; Cornell University Press: Ithaca, NY, 1979.
(34) Broutin, I.; Ries-Kaut, M.; Ducruix, A. *J. Appl. Crystallogr.* **1995**, *28*, 614.
(35) Nemethy, G.; Scheraga, H. A. *J. Chem. Phys.* **1964**, *41*. 680.
(36) Doi, M. Edwards, S. F. *Theory of Polymer Dynamics*; Clarendon Press: Oxford, U.K., 1986.
(37) Mukherjee, M.; Nambissan, P. M. G.; Chakravorty, D. *Phys. Rev. B* **1998**, *57*, 848.

MA061745D